ISTITUTO NAZIONALE DI FISICA NUCLEARE

Sezione di Trieste

INFN/AE-94/19

7 settembre 1994

L. Lanceri and G. Vuagnin

A SCINTILLATING-FIBER HODOSCOPE WITH MULTI-ANODE PHOTOMULTIPLIER READOUT

Servizio Documentazione
dei Laboratori Nazionali di Frascati

A scintillating-fiber hodoscope with multi-anode photomultiplier readout

L.Lanceri[1,2] and G.Vuagnin[1,2,3]

September 25, 1994

Abstract

Position sensitive photomultipliers coupled to scintillating fibers allow the construction of compact and fast particle tracking detectors. We describe a detector based on these techniques, and discuss its measured performances. Efficiency, space resolution and the effects of cross-talk between neighbour channels are studied in detail.

(To be submitted to Nuclear Instruments and Methods.)

[1]Dipartimento di Fisica, Universita' di Trieste, Via A. Valerio 2, I-34127 Trieste, Italy
[2]INFN, Sezione di Trieste, Via A. Valerio 2, I-34127 Trieste, Italy
[3]Present address: CERN, SL Division, CH-1211 Geneva 23, Switzerland

1 Introduction

With the recent development of position-sensitive photomultipliers (PSPM) [1], pioneered by the work of Kuroda [2], charged particle detectors based on scintillating fibers offer several advantages.

The combination of plastic scintillator and photomultiplier retains the well known characteristics of low noise, large gain, good linearity and time resolution. Fibers add position measurement, and PSPMs, whose photocathode segmentation is well matched to millimetre-diameter fibers, offer an important reduction in size, cabling and cost per channel with respect to conventional single-channel photomultipliers.

A possible drawback of PSPMs is the unavoidable, to some extent, cross-talk between neighbour channels. Several authors [3] have studied ways of turning this disadvantage into a tool for position reconstruction. PM manufacturers have however been studying ways of reducing this effect. The amount of cross-talk is therefore an important parameter that must be well known and taken into account in the detector design.

In this article we present a scintillating-fiber hodoscope recently built at INFN-Trieste for the XLHB/RD22 experiment [4] and tested at CERN. Experimental results on efficiency, space resolution and cross-talk effects are presented and compared with the expectations from a simulation of the detector. Indications on ways of optimising the detector performances in future designs are given.

2 Description of the hodoscope

The hodoscope was designed as part of a telescope for the detection of high energy protons extracted from the CERN SPS by channeling in a bent crystal [4]. The initial requirements were: an active area of about $10 \times 10\text{cm}^2$, a space granularity of approximately 1 mm, ability to stand high rates and good time resolution. These properties were needed to distinguish single channeled particles from background particles and correlate their signals with those of other detectors for the measurement of their direction.

The multi-anode photomultiplier XP1724 [5] was chosen because of its relatively low cross-talk between neighbour channels: less than 5% according to the manufacturer. The number of photocathode pixels (96) and their size (2.54×2.54 mm^2) are well matched to the characteristics of the hodoscope outlined above.

Two prototype hodoscopes were built. Their mechanical structure is shown in figure 1. The desired space coverage and resolution is obtained by arrays of scintillating fibers, each being 1 mm in diameter. The detector efficiency for minimum ionising particles is maximised by superimposing several layers of fibers, to eliminate dead spaces and increase the light output per incident particle. To minimise background rates, the active area is restricted by gluing each scintillating fiber, 10 cm long only, to a clear fiber, 20 cm long, that acts as a passive light guide reaching the PM photocathode window. Both types of fiber (from Bicron, BCF-12 and BCF-98) are coated by the manufacturer with white EMA (extra-mural absorber) to avoid cross-talk. The free end of the scintillating fibers are polished and covered with an aluminium sheet to improve light collection.

The first prototype was made of four layers of 48 fibers each, carefully positioned by gluing on thin epoxy plates grooved at 1.1 mm steps. Each layer was shifted with respect to the neighbours by 0.25 mm, to obtain the cross-section shown in figure 2. The total

active surface was about 5×10 cm^2. Groups of four fibers were formed as indicated in the figure, to be read-out by a single PM pixel. Of the 96 pixels of a PM one half (48) were therefore used.

The total thickness of active scintillating fiber crossed by incoming particles at right angle with the detector plane is shown in figure 3 as a function of the position: the minimum is about 2.5 mm if neighbour pixels are added together.

The second prototype counter has similar characteristics; its sensitive area is about 10×10cm^2, and all the 96 PSPM pixels are used for the read-out.

3 The detector read-out

The Philips XP1724 photomultiplier [5] has an input window made of optical fibers and a bialkali photocathode segmented in 96 pixels of 2.54×2.54 mm^2 each. The groups of four fibers (figure 2) were coupled to PM pixels as shown in figure 4.

The PM base implemented the recommended voltage divider so that the segmented output electrode operated as a dynode and the 96 output signals were positive. They were brought by coaxial cables to four "scotchflex" connectors, mounted on printed circuits with the 96 individual 1 KΩ load resistors.

The signals were inverted by pulse transformers mounted on separated boards, kept close to the PM base. Multi-coaxial 50Ω flat cables carried the negative signals to the read-out electronics. For the short space (0.5 m) between the PM and the inverters 100Ω twisted pair cables were used, without significant deterioration of the signal quality.

For all the exploratory studies described in this article the hodoscope signals were digitised by LeCroy charge integrating ADCs (LRS2282A, 0.25 pC/ADC count), in order to obtain the maximum possible amount of information. In many applications, including ours, discrimination and pulse counting by scalers can be used instead.

Typical signals obtained with electrons from a radioactive beta source are shown in figure 5. The typical PM gain is sufficiently high, about 5×10^6, so that for most purposes further electronic amplification is not needed.

4 Experimental set-up

The hodoscope was tested both in the laboratory and on a high energy beam at CERN.

4.1 Mapping the PM response with a LED

The photomultiplier response was tested in the simple set-up shown in figure 6. A light emitting diode was used as pulsed light source. It was coupled to the PM by a clear fiber (Bicron BCF-98) of 1 mm diameter that could be positioned in front of the centre of each pixel by a precisely machined mask. The signals at the PM output were both checked at the scope and digitised by charge-integrated ADCs to obtain a map of the response of the PM pixels and of the cross-talk (section 5.1).

4.2 Tests with a radioactive source

A preliminary test with minimum ionising particles in the laboratory was obtained with the apparatus sketched in figure 7. A ^{106}Ru beta source was collimated by a Plexiglas screen with a 3 mm diameter hole. The scintillation counter S ($1.5 \times 1.5 \times 0.3$ mm^3), was viewed by two photomultipliers. Their signals in coincidence defined the trigger, gating the charge-integrating ADC LRS2282 used to digitise each of the signals from the hodoscope. Data were read via a CAMAC interface and analysed by an on-line personal computer. Scalers were also used to monitor trigger rates.

4.3 Tests with a high energy particle beam

The hodoscope prototype was finally tested at CERN in a high-energy electron beam ($X3$, 50 GeV/c electrons) taking data parasitically during a calibration run of a calorimeter for the DELPHI experiment. The set-up is shown in figure 8. Two trigger counters, T_1 and T_2, were used in coincidence to define an active area of 2.5×2.5 cm^2.

Three proportional wire chambers with delay line read-out (DWC, Delay line Wire Chamber [6]) were used to measure the incoming particle tracks and predict their position and angle of incidence on the hodoscope under test. DWC data were digitised by CAMAC TDCs; the space co-ordinate could be obtained, after calibration, from the difference of the times of arrival of the signals from the two ends of each delay line; for single hits the sum of the two times is constant. The space resolution of these chambers, about 300μm, is perfectly adequate for efficiency studies, but not optimised for studies of a hodoscope space resolution of the same order of magnitude. An estimate can be obtained however by unfolding the space resolution of the tracking chambers from the experimental distributions.

Each hodoscope pixel was connected to a CAMAC charge integrating ADC. All data were recorded by a Fastbus processor on remote discs via a local network, to be later analysed off-line.

5 Experimental results

5.1 Light output and photocathode uniformity

A preliminary study of the hodoscope light output and of the photocathode response uniformity was performed in our laboratory. The absolute gain of the XP1724 photomultiplier was also evaluated.

The hodoscope light output was measured by a conventional XP2020 photomultiplier, for electrons emitted by the ^{106}Ru beta source, crossing the detector and the trigger scintillation counter S. The charge scale of the XP2020 output was calibrated by the single photo-electron pulse charge distribution (figure 9(b)), obtained triggering at random the photomultiplier on its noise, mainly contributed by single photo-electrons leaving the cathode after thermal emission. The average signal (figure 9(a)) corresponds to about 20 photo-electrons.

A map of the relative gain of the XP1724 pixels was obtained by the apparatus described in section 4.1. The average responses are shown in figure 10(a) for the 48 pixels used by the hodoscope prototype. A variation by a factor up to about 3 was observed.

In figure 10(b) the average pattern of cross-talk observed around each pixel is shown. Typically it was about 10%.

The measurement of the hodoscope response to particles from the collimated beta source was repeated using the XP1724 as photon detector, with each pixel coupled to a group of four fibers. As an example, the distribution of the sum Σ of the signals from three contiguous channels including channel 24, for events in which it had the maximum signal, is given in figure 11(a). The position of the hodoscope channel giving maximum signal is well correlated with the collimated source (figure 11(b)). The mean XP1724 output charge is about 64 ADC counts, corresponding to 16 pC. Taking into account the average number of p.e. (20) observed by the XP2020 PM and assuming the two PMs have similar photocathode quantum efficiencies, the XP1724 gain is estimated to be about 5×10^6, as expected.

5.2 Efficiency

The efficiency of the scintillating fiber hodoscope was studied analysing data taken at the CERN test beam. Clean single track events were selected by requiring one hit per DWC, fitting a straight line to the three hit co-ordinates with good χ^2, ($\chi^2 < 6$) and checking, after careful alignment, that the track crossed the active area of the detector.

For efficiency studies, after pedestal subtraction the pixel with maximum pulse height was looked for. The sum of its signal with that of the two neighbour groups of fibers was formed, to obtain the total signal when the track is crossing fibers connected with different pixels. The distribution of these three-fold sums is shown in figure 12 for events in which a single clean track is found by the criteria outlined above. The peak, corresponding to single minimum ionising particles, is well separated from the noise.

The hodoscope efficiency can be estimated as the fraction of single-track events satisfying the following criteria: a charge threshold is required when looking for the hodoscope channel with maximum signal, and its central co-ordinate is required to be within 2 mm of the track intercept, reconstructed from DWC data. Figure 13 shows the average efficiency as a function of the threshold, expressed in ADC counts (1 ADC count = 0.25 pC).

The efficiency for a given threshold can be plotted as a function of the position of the reconstructed track intercept. In figure 14 the position dependence of the efficiency is shown for two values of the threshold. At low threshold (5 ADC counts corresponding to 1.25 pC) the efficiency is about 98% and independent of the position. At higher threshold (45 ADC counts) the periodic structure of the fiber groups determines the position dependence of the efficiency: more details on these effects are given in the following sections.

5.3 Position reconstruction and space resolution

A simple estimator of the x co-ordinate of the incident particle is the centre of the interval covered by the group of fibers giving maximum signal. The distribution of the difference of this estimate with respect to the co-ordinate x_{DWC}, measured by the intercept of the straight line fitting the co-ordinates measured by the DWCs, is given in figure 15. Unfolding the space resolution of about 200μm, due to the DWC measurement, a resolution of approximately 490μm can be assigned to the measurement based on the hodoscope.

An improvement in space resolution can be obtained in principle using the available information on the pulse height from each hodoscope channel. However, position estimators based on weighted averages suffer from the fluctuations in pulse heights, dominated by the rather small number of primary photo-electrons: as a result the improvement turns out to be marginal.

5.4 Cross-talk effects

Cross-talk between neighbour XP1724 pixels has been studied by plotting the average pulse height from each hodoscope channel (i=1,24) as a function of the position x_{DWC} of the incoming particle, reconstructed by DWCs (figure 16(a)).

A cross-talk of about 10%, compatible with the LED measurement described in section 5.1, appears in each channel when the incoming particles cross a group of fibers connected to neighbour pixels.

In figure 16(b) this is shown for one hodoscope channel ($i = 17$) as an example. The lower peaks correspond to the signal from particles crossing the two channels ($i = 4$ and 23), connected to neighbour pixels (figure 16(c)).

6 Comparison with simulations

The response of the detector to minimum ionizing particles was simulated by a Monte Carlo program with a model including the following effects:

- thickness of scintillating material crossed, as a function of the position of the track;
- statistical Poisson fluctuations of the number of primary photo-electrons (p.e.); an average of 7 p.e./mm was assumed, according to the measured light yield (section 5.1);
- Poisson fluctuations in the number of secondary electrons extracted in each dynode of the photomultiplier chain;
- cross-talk between neighbour pixels, taken as a fixed 10%, independently of the geometrical details of the coupling of groups of four fibers to one pixel;
- in order to compare the predictions of the model with the experimental data from the test beam, the DWC resolution in defining the position of the track is taken into account as a gaussian smearing with 200μm rms.

As an example, figure 17 shows the comparison between the measured average signals from three neighbour hodoscope channels, as a function of the reconstructed track position x (figure 17(b)), and the results obtained from the simulation program (figure 17(a)).

The agreement between experimental data and our model is fair; it may still be improved by a more refined description of the effects of the cross-talk, affecting the tails of the distributions (figure 17). The Monte Carlo program, tuned on experimental data, is a useful tool in understanding the prototype detector performance and in designing future optimized versions of the detector.

In applications in which it is needed, a significant improvement in space resolution can be reached both by a different arrangement of fibers [8] and by reducing the fluctuation

in the number of primary photo-electrons. This can be obtained by improving the light yield of the scintillating material and aspects of the photon collection efficiency related to the mechanical construction of the hodoscope. The photon-electron conversion efficiency, on the other hand, can only be improved by using different photon-sensitive devices [7].

7 Conclusions

A prototype hodoscope made of four layers of closely packed 1 mm diameter scintillating fibers, read-out by an XP1724 position sensitive photomultiplier, has been built and extensively tested.

The average efficiency for minimum ionising particles was measured to be larger than 98%, with a charge threshold of 1.25 pC, and the space resolution about 490μm for a simple estimator using only part of the available information.

The cross-talk between neighbour pixels of the XP1724 PSPM was measured to be of the order of 10%; the PSPM was routinely operated in conditions corresponding to a gain of about 5×10^6.

The detector perfomance was interpreted by a Monte Carlo simulation that describes the experimental data satisfactorily and can be used to optimize the detector design.

Acknowledgements

We gratefully acknowledge the technical skill of G.Venier, S.Reia and D.Iugovaz (INFN Trieste) in the construction of the hodoscope prototype. We are indebted to prof. Busso (INFN Torino) who provided the printed circuit of the XP1724 voltage divider. Finally, we would like to thank our colleagues of the DELPHI group, in particular T.Camporesi, V.Cassio, G.Della Ricca and E.Vallazza for their help during the data taking on the test beam, and P.Poropat for useful comments and discussions.

References

[1] Photomultiplier tubes: multi-channel tubes, Philips Photonics.
Photomultiplier tubes: multi-anode tubes, Hamamatsu Photonics.

[2] K.Kuroda, D.Sillou and F.Takeuchi, Rev. Sci. Instr. 52 (1981) 337.

[3] K.Kuroda et al., Nucl. Instr. and Meth. in Phys. Res. A300 (1991) 259-267.

[4] H.Akbari et al., Phys. Lett. B313 (1993) 491-497.

[5] Photomultipliers tubes: XP1724, Philips Photonics.

[6] A.Manarin and G.Vismara, CERN Internal Report LEP/BI-TA/Note 85-3.

[7] M.Atac et al., Nucl. Instr. and Meth. in Phys. Res. A320 (1992) 155-160.

[8] R.Battiston et al., Nucl. Instr. and Met. in Phys. Res. A238 (1985) 35-44.

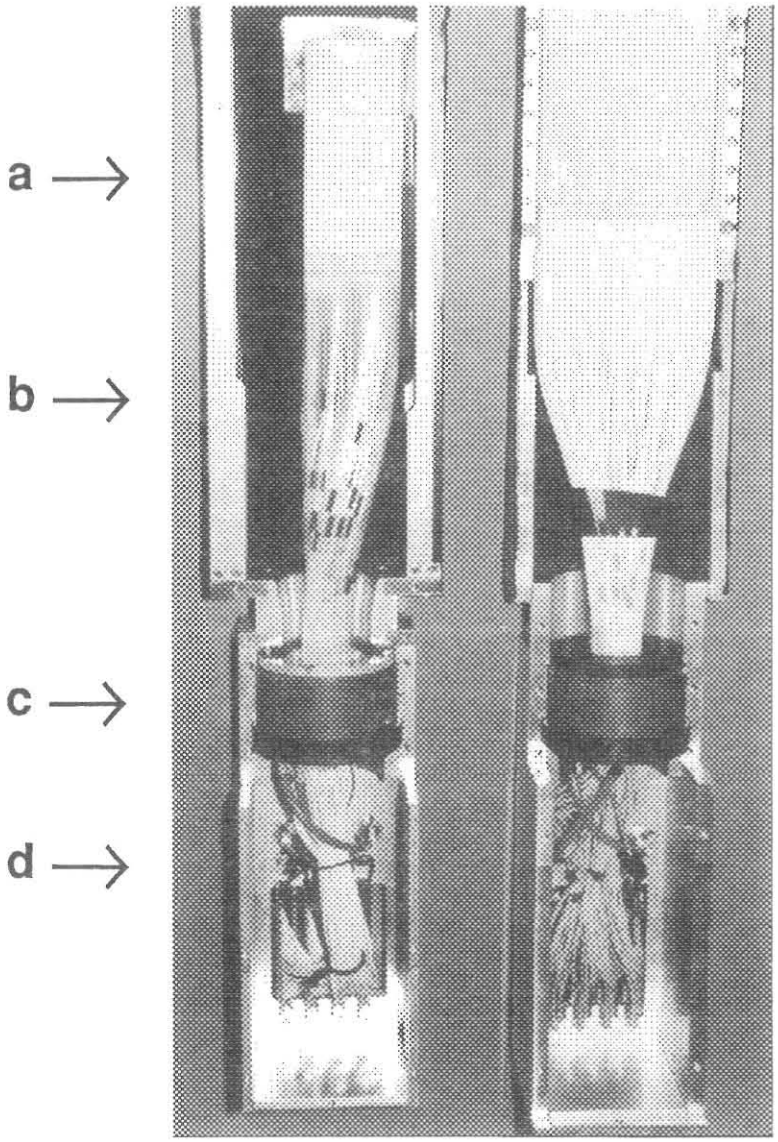

Figure 1: Mechanical structure of the two hodoscope prototypes: (a) scintillating fibers; (b) clear fibers; (c) XP1724 photomutiplier; (d) base with high-voltage and signal connectors.

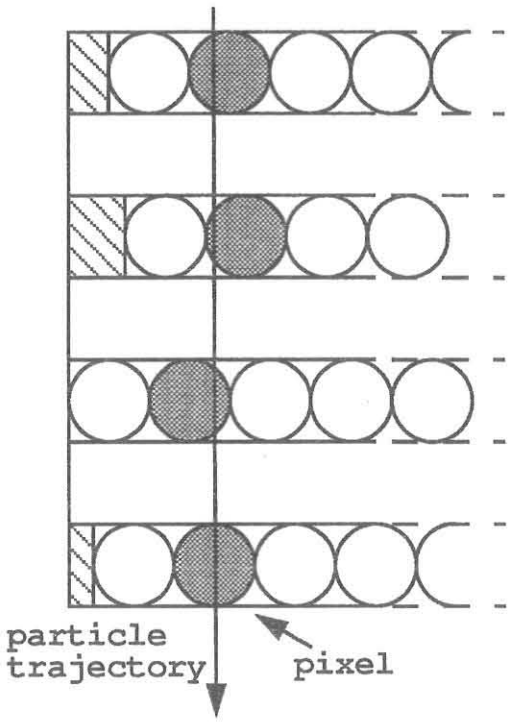

Figure 2: Cross-section of the hodoscope, with grouping of fibers for pixel readout.

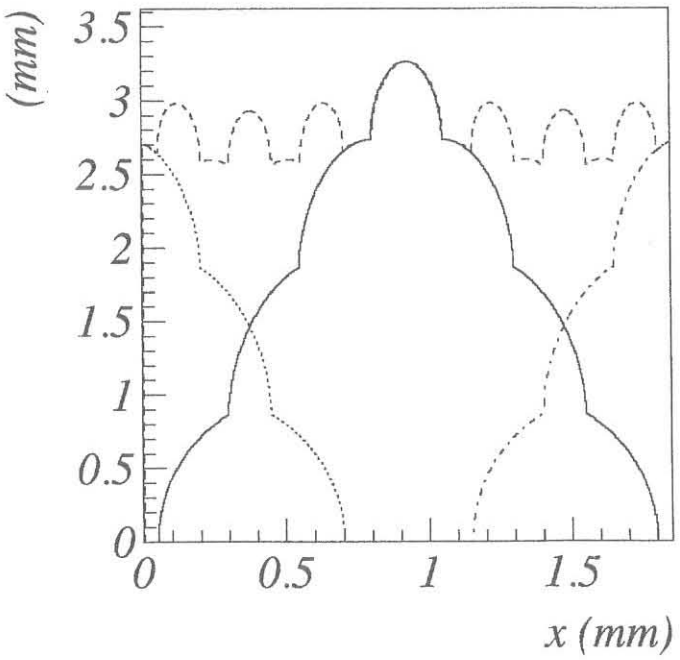

Figure 3: Total thickness of fiber normally crossed by a particle for three neighbour pixels (continuous, dotted and dashed-dotted lines) and their sum (dashed line), as a function of the position x, defined in figure 17(c).

				48	47						
			41	42	43	44	45	46			
		40	39	38	37	36	35	34	33		
	23	24	25	26	27	28	29	30	31	32	
	22	21	20	19	18	17	16	15	14	13	
1	2	3	4	5	6	7	8	9	10	11	12

Figure 4: Correspondence between groups of fibers and PM pixels.

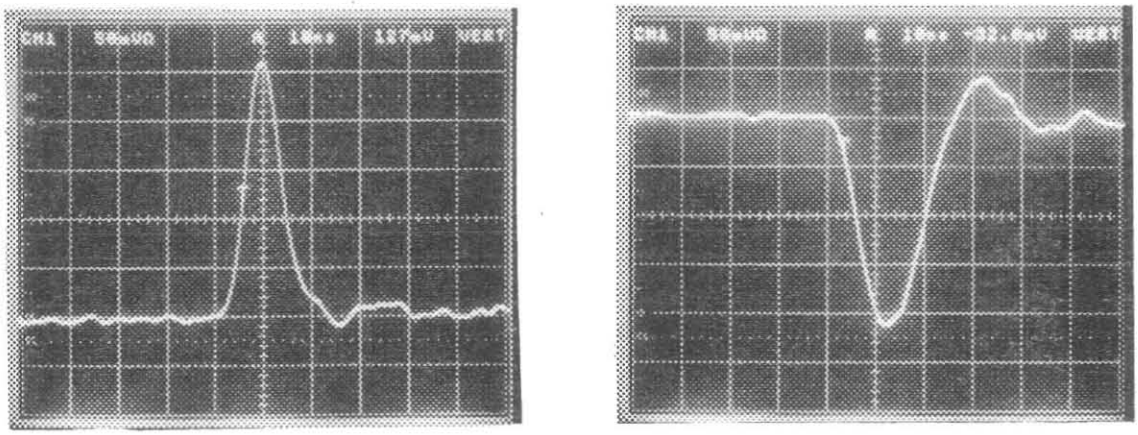

a) b)

Figure 5: Typical signal obtained by minimum ionising particles: (a) at the PM output; (b) after inversion by the pulse transformer.

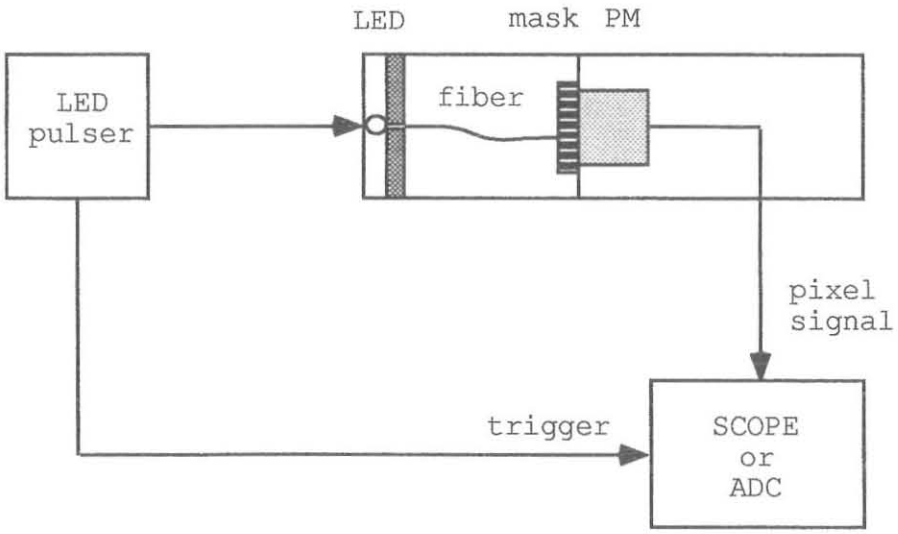

Figure 6: Set-up for PM response measurement.

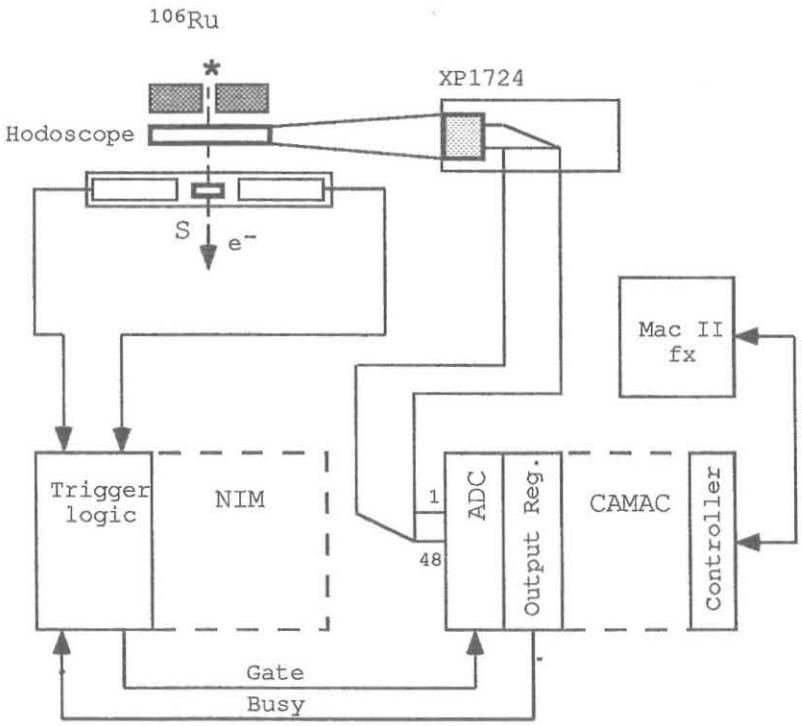

Figure 7: Set-up for measurements with a radioactive beta source.

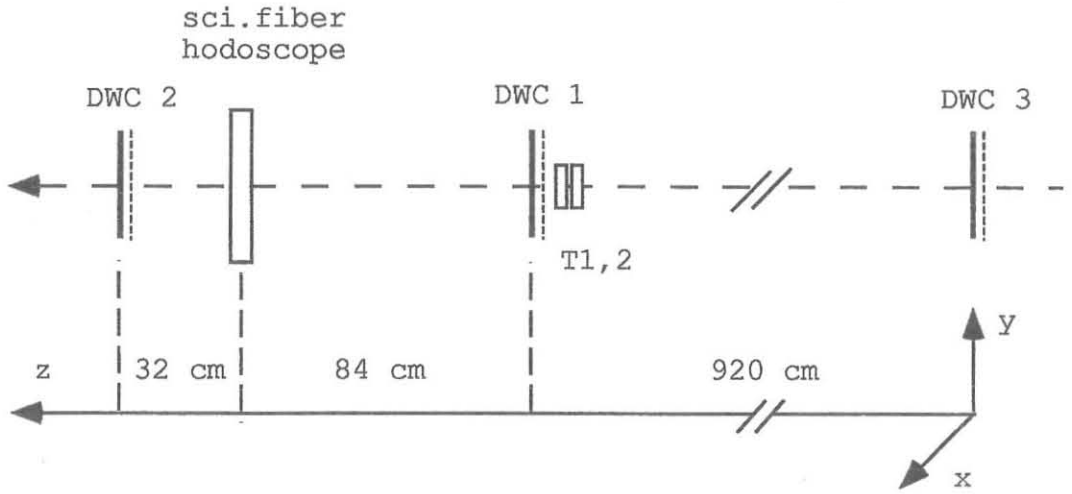

Figure 8: Set-up for measurements in the test beam X3 at CERN.

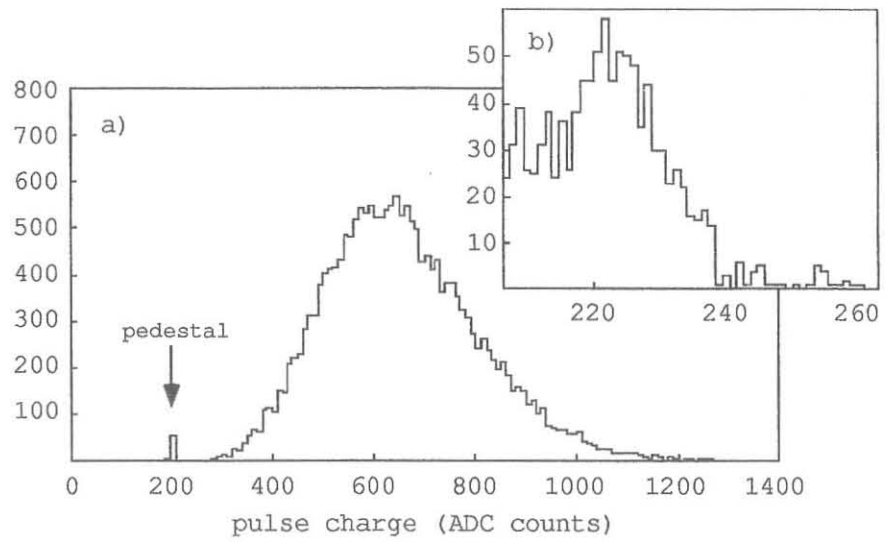

Figure 9: (a) Distribution of the pulse charges (in ADC counts) of a XP2020 photomultiplier coupled to the hodoscope crossed by electrons from the ^{106}Ru beta source. The average corresponds to about 20 photo-electrons, if the scale is calibrated by the single photo-electron spectrum (b).

a)

				.35	.45					
			.60	.60	.55	.30	.35	.37		
		.60	.65	.80	.60	.65	.90	.90	.75	
	.65	.80	.80	1.0	.80	.70	.65	.90	.90	.75
	.85	.90	.95	1.0	.90	.90	.75	.50	.40	.48
.85	1.0	1.0	.95	1.0	.90	.90	.70	.45	.40	.40	.35

b)

5	10	5
10	100	10
5	10	5

Figure 10: Measured response of the XP1724 PSPM pixels: (a) average pulse height obtained with the LED pulser (arbitrary units); (b) typical cross-talk pattern, normalised to the pulse height measured in the central pixel, illuminated by LED pulses as described in the text.

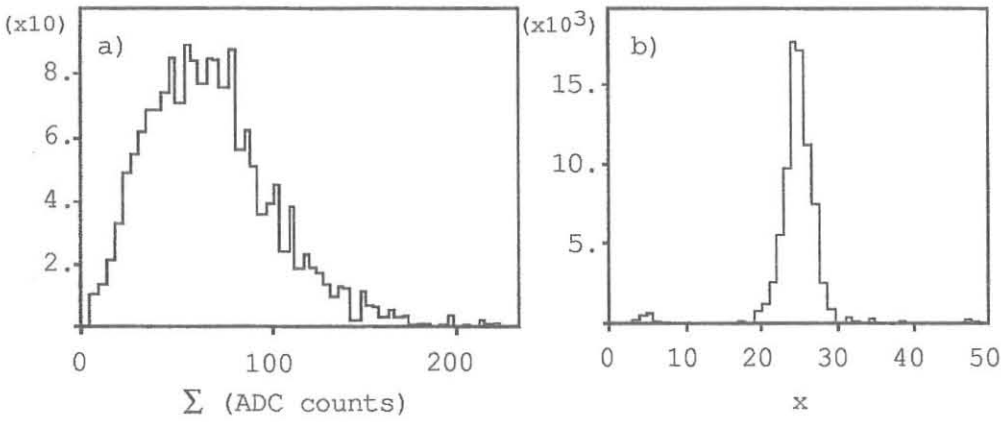

Figure 11: (a) Distribution of the sum Σ of the pulse charges (in ADC counts) collected from groups of three neighbour channels, centered around channel 24, when it is giving the maximum signal; (b) distribution of the position x of the hodoscope channel giving maximum signal when exposed to the collimated beta source; x is expressed as an integer multiple of the hodoscope pitch (1.1 mm).

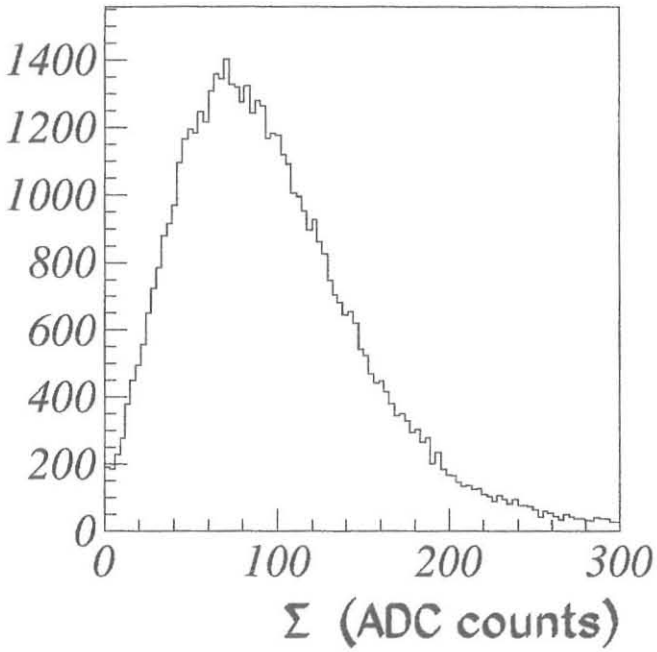

Figure 12: Distribution of the sum of the pulse charges (in ADC counts) of groups of three neighbour channels, including in each event the one with maximum signal, after pedestal subtraction in each channel. Data are from high energy electrons (test beam).

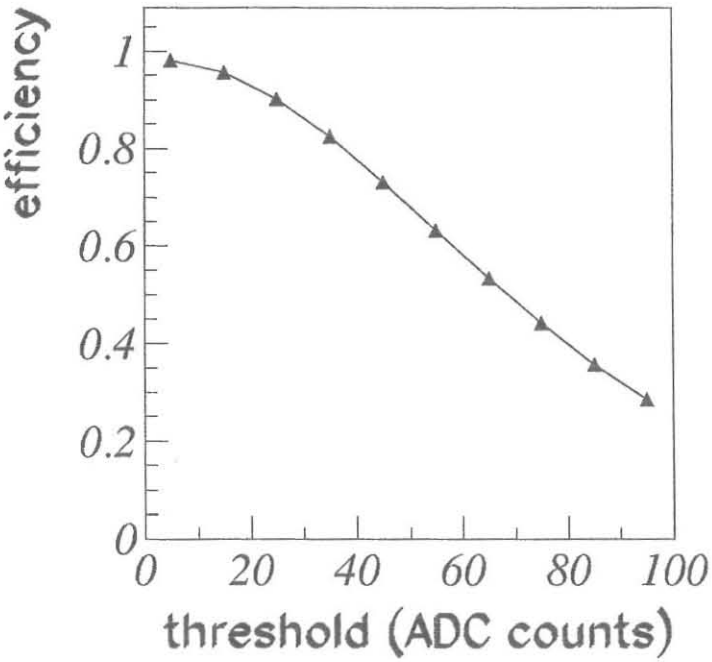

Figure 13: Hodoscope average efficiency as a function of the threshold, expressed in terms of ADC counts.

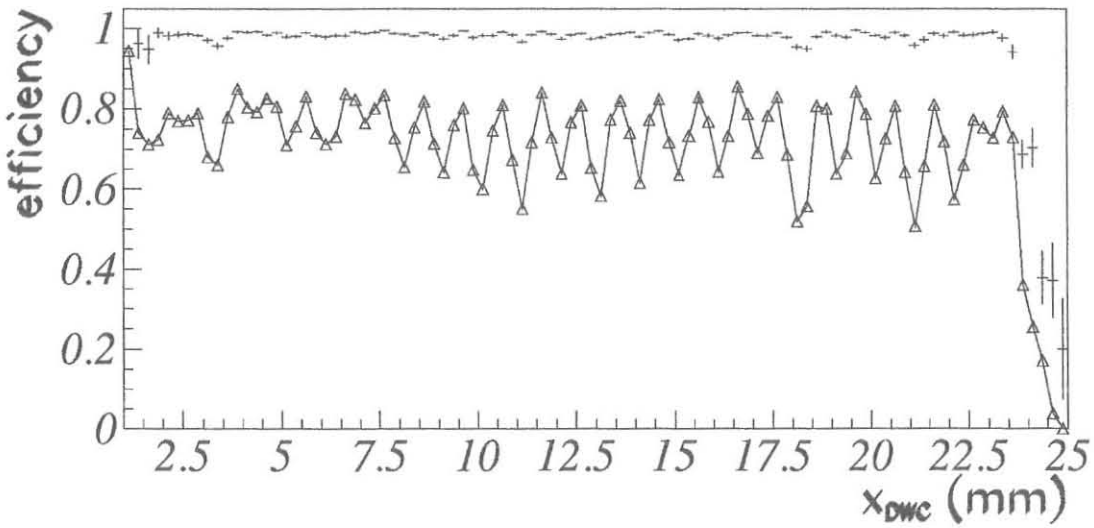

Figure 14: Hodoscope efficiency as a function of the track position for two values of the threshold (5 and 45 ADC counts). Triangles joined by a line correspond to the higher threshold.

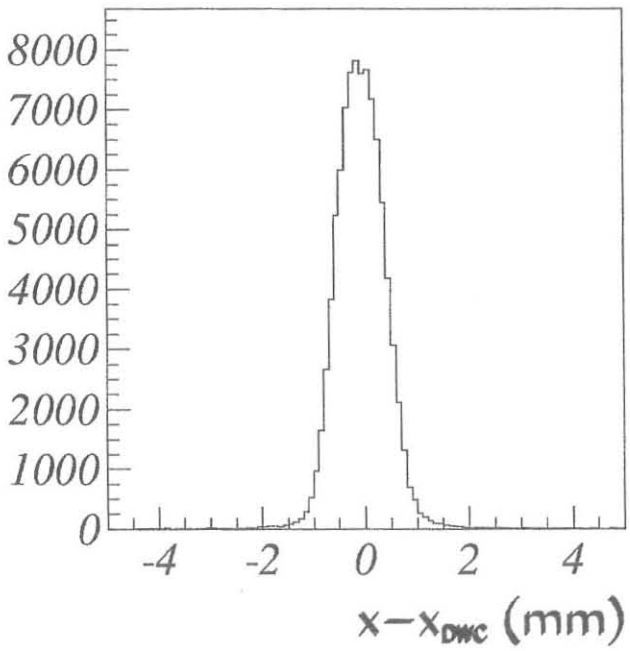

Figure 15: Distribution of the difference $x - x_{DWC}$ of the co-ordinate of the incident particle estimated using the hodoscope and the DWCs, as explained in the text.

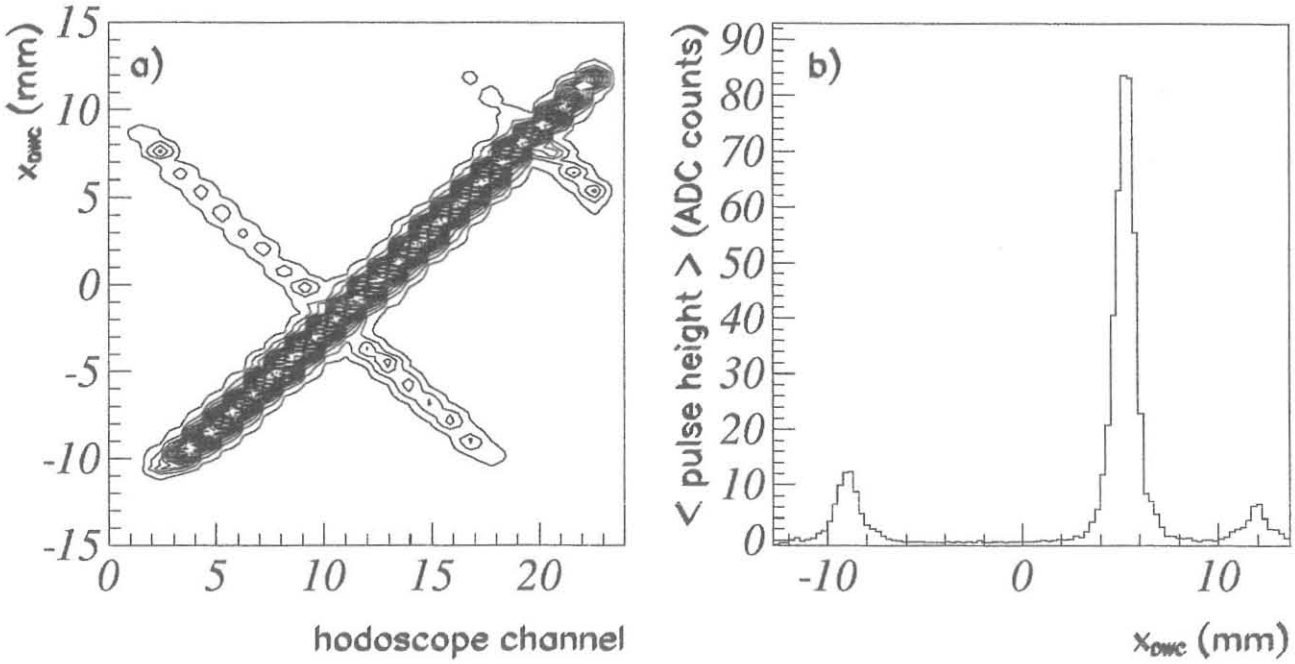

c)

					24	23	22	21	
11	12	13	14	15	16	17	18	19	20
10	9	8	7	6	5	4	3	2	1

Figure 16: (a) Contour plot of the average pulse height for hodoscope channels $i, i = 1, 24$ as a function of the position x_{DWC} of the incoming particle, reconstructed by DWCs; 30 contour levels are shown, equally spaced in the full range; (b) projection of one slice ($i = 17$) onto the x_{DWC} axis; (c) correspondence between PM pixels and the 24 hodoscope channels crossed by the test beam particles.

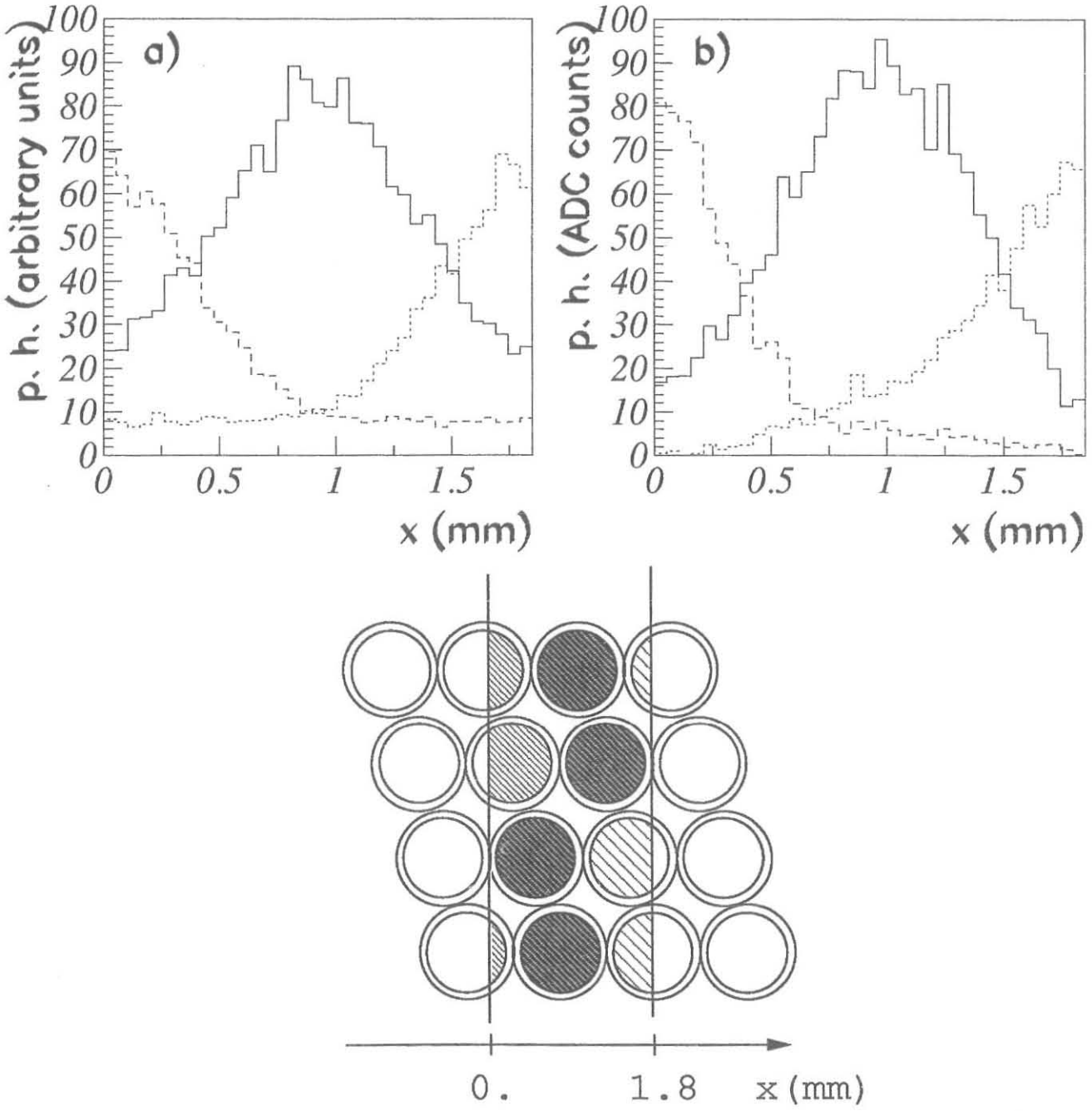

Figure 17: (a) Simulated average response of the detector as a function of the track position x including all the effects described in the text; (b) experimental distribution of the average pulse height from three neighbour hodoscope channels, as a function of the reconstructed position x of the incoming particle; (c) geometry of one detector cell including a full group of four fibers and fractions of the two neighbour groups.